

**Inter-Spin State Transition associated with magnetization jump in
 $\text{Y}_{0.33}\text{Sr}_{0.67}\text{CoO}_3$**

Yufeng Zhang, Ayako Yamamoto and Mitsuru Izumi

**Laboratory of Applied Physics, Tokyo University of Marine Science
and Technology, 2-1-6, Etchujima, Koto-ku, Tokyo 135-8533, Japan**

E-mail: yzhang@e.kaiyodai.ac.jp

(Received 2005)

We study the crystal structure, electrical resistance and magnetic properties on the perovskite-based $\text{Y}_{0.33}\text{Sr}_{0.67}\text{CoO}_3$ oxides. Two kinds of Co-O clusters form the layered structure with CoO_6 octahedron and CoO_4 tetrahedral polyhedron in alternate order. $\text{Y}_{0.33}\text{Sr}_{0.67}\text{CoO}_3$ shows a Curie temperature at 304 K and subsequently exhibits a DC magnetization jump (T_J) around 200 K with a thermal hysteresis under 0.01 T. The thermal hysteresis becomes small and disappears with increasing the applied magnetic field and the T_J shifts to lower temperature. We interpret that the inter-spin state transition, from low to intermediate spin state occurs in the orbital ordering state Co^{3+} ions formed at 304 K. This results in the magnetization jump and the high external field decreases the low ordered temperature and T_J shifts to lower temperature. The magnetization jump of

air-processed sample is larger than that of O₂-processed sample and the T_J is higher than that of under the same magnetic field. We interpret the rich Co³⁺ ions and the high orbital ordering state coming from the oxygen deficiency increase the magnetization and the T_J .

PACS number(s): 75.60.Ej, 75.30.Sg, 75.25.+z, 71.70.Ej

1. Introduction

The transition-metal oxides with perovskite-type structure ABO_3 have been extensively studied because of their rich physics and potential application in their behaviors of electrical transport and magnetic properties. The rare-earth strontium cobaltites $RE_{1-x}Sr_xCoO_3$ (RE is the rare-earth ion) have received lots of attention due to a couple of unique properties; namely, the existence of different Co spin state¹⁻³, i.e, high-spin state, intermediate spin state, low spin state with different S , as well as the unusual magnetic ground state of doped cobaltites⁴⁻⁶. The transition of high-spin state to low spin-state state occurs in many cobaltites⁷⁻⁹ such as $Pr_{0.5}Ca_{0.5}CoO_3$ ⁷, while the “intermediate spin-state”, which is the seldom observed in Co compounds, has been claimed to exist in $La_{1-x}Sr_xCoO_3$ ¹⁰⁻¹¹. The cobaltites can have Co-O octahedral, tetrahedral or both structures depending on the amount of oxygen present¹²⁻¹³. The physical properties of these materials are strongly dependent upon composition as well as ionic and oxygen vacancy ordering. Oxygen ionic conductivity, for example, is known to be affected by oxygen vacancy ordering and associated structure relaxation¹⁴; magnetic behavior will be affected by the Co^{3+}/Co^{4+} ratio and distribution⁹. We prepared $Y_{0.33}Sr_{0.67}CoO_3$ samples processed under air and oxygen conditions respectively by the conventional ceramic technique, which results in different oxygen concentration and so as to the sample magnetic

properties. Y^{3+} ion is ideal for the studies as Y is non-magnetic and a small ionic size (Y^{3+} ion size is 1.075 Å, and La^{3+} ion size is 1.216 Å). Power X-ray diffraction (XRD) of the samples and Rietveld refinement showed formation of single phase compounds and perovskite structure with space group I4/mmm, which is consistent with previous results^{12, 15}. In the field cooling magnetic measurement, there is a DC magnetization jump around 200 K which indicates the spin state transition from low to intermediate spin state.

2. Experiments

Polycrystalline samples of $\text{Y}_{0.33}\text{Sr}_{0.67}\text{CoO}_3$ with O_2 -processed and air processed were synthesized from stoichiometric mixtures of SrCO_3 (99.999%), Co_3O_4 (99.9%) and Y_2O_3 (99.99%) by the conventional solid state method. The mixtures were ground, pressed into a pellet and calcined at 1100 °C for 48 h in O_2 . The product was reground, pressed into a pellet and finally sintered at 1250 °C under flowing oxygen for up to two days until no further reaction was evident by the X-ray powder diffraction. The air-processed sample was prepared in air under the same temperature condition. Room temperature measurements were done by the RADII-A diffractometer and Cu K_α radiation and refinement of the diffraction data was done using the Rietveld power diffraction profile fitting technique¹⁶. Magnetization was measured by Quantum Design SQUID magnetometer in

the temperature range of 5 K to 400 K and the magnetic field of 0 T to 5 T. DC electrical resistance was measured by a four-probe method down to 10 K.

3. Results and Discussion

Power XRD patterns and Rietveld refinement for O₂-processed Y_{0.33}Sr_{0.67}CoO₃ sample reveal an existence of the tetragonal structure with a space group of I4/mmm (139) and a layered ordering of oxygen vacancies. The lattice parameters are $a = 7.6164(2)$ Å and $c = 15.2747(5)$ Å. There are two asymmetry occupations for the Co cations, Co1 and Co2. Two kinds of Co-O clusters form the layer structure with CoO₆ octahedron and CoO₄ tetrahedral polyhedron in alternate order, which is consistent with the literature^{12, 15}. There appears an impurity phase of Y₂O₃ about 29°, which haven't influence on the magnetic memory effect. Observed and calculated patterns are shown in Fig. 1. Crystal and refinement data are given in Fig. 2 and Table 1. Here we take O₂-processed Y_{0.33}Sr_{0.67}CoO₃ as an example and refer to the neutron diffraction analysis result¹⁵. Y ionic size is close to Sr ionic size, so some Y and Sr site ions are difficult to distinguish from the only XRD data, same with the neutron diffraction analysis. Table 1 also shows the lattice parameters for air-processed sample are larger and the average Co2-O bond distance is longer than those for O₂-processed sample. However the average Co1-O bond distance is shorter than that for

O_2 -processed samples. From these, we can see the effect of oxygen non-stoichiometry^{9, 17}. The air-processed sample implies the lower oxygen content and different distortion, which may influence the different magnetic and electrical properties^{12, 17}.

Fig. 3(a) shows the magnetization versus temperature data of O_2 -processed $Y_{0.33}Sr_{0.67}CoO_3$ sample under an applied field of 0.01 T. There is a DC magnetization jump (T_J) around 180 K with a thermal hysteresis, which is that the magnetization normally returns to the high temperature after the jump of magnetization in the field cooling, indicating a kind of magnetic memory effect. To our knowledge, it is firstly reported in $Y_{0.33}Sr_{0.67}CoO_3$ samples. This phase transition is most likely due to the spin state transition of Co^{3+} from low to intermediate spin state and magnetization drop instantly. With increasing temperature another transition is seen at 304 K, which is the Curie temperature T_C , defined as the maximum of $-DM/DT$. We interpret this is due to the orbital ordering state Co^{3+} competition between superexchange antiferromagnetic and ferromagnetic interaction. Same phenomena appear in the air processed sample (see Fig. 3(b)). They have the same high transition temperature about 304 K, however the magnetization increases and T_J is higher. An increase of Co^{3+} ion in the air processed sample exhibits a bigger magnetization and a higher order temperature.

As shown in Fig. 3(c), the magnetization jump of the O₂-processed sample slowly vanishes and the relative jump temperature T_J shifts to the lower temperature from 180 K at 0.01 T to 164 K at 1 T. It indicates the “melting” of the orbital ordered antiferromagnetic state and the decrease of low ordered temperature, a fact well documented for manganites¹⁸. However, the T_C does not change and it is around 304 K. Fig. 3(c) also shows the magnetization increase near low temperature with the applied field increasing, which is an existence proof of the antiferromagnetic state.

Figure 4 shows zero-field cooled (ZFC) magnetizations for a polycrystalline sample of O₂-processed Y_{0.33}Sr_{0.67}CoO₃ versus temperature in an applied magnetic field of 0.01 T and 0.5 T, respectively. There is a cusp at about 304 K near T_C , which is sometimes related to glassiness⁸ or spin glasslike¹⁹. With the magnetic field increasing to 0.5 T, the cusp temperature is still around 304 K, which suggests the cusp should be attributed to glassiness^{5, 20} and magnetocrystalline anisotropy¹⁹. The competition of Co³⁺ ferromagnetic interaction and antiferromagnetic superexchange interaction induces the appearance of the cusp, i. e, the system appears to contain ferromagnetic clusters in an antiferromagnetic matrix¹⁷.

For the studying the character of the difference magnetic transition temperature, we measured magnetization versus applied field curve for air-

processed sample at 295 K, 210 K and 10 K, for O₂-processed sample at 285 K, 190 K and 10 K, as is shown in Fig. 5(a) and (b). The existence of the hysteresis loop for air-processed sample at 295 K and 210 K implies a ferromagnetic component, suggesting a ferromagnetic material. The lack of saturation will relate to the antiferromagnetism¹⁷. The ferromagnetic clusters within an antiferromagnetic matrix are the most likely model here. There is no hysteresis loop for air-processed sample at 10 K and for O₂-processed sample at every temperature implies the existence of an antiferromagnetism. The magnetization curve shows the sample ferromagnetism. So it makes true that ferromagnetic clusters are within an antiferromagnetic matrix.

We measured the electrical resistance versus 1000/T curve at a zero field down to 115 K below room temperature. The results of both samples show the thermal activation-type which suggests nonmetallic insulator. The obtained activation energies are approximately 0.33 eV of air-processed sample and 0.6 eV of O₂-processed sample below room temperature. The normalized electrical resistance and the electronic energy of air-processed sample are smaller than those of the O₂-processed sample. For air-processed sample, a high orbital ordering state and the decrease of the average Co1-O bond distance reduce the thermal activation electronic gap and electrical resistance, similar to Korotin et. al. calculated results²¹ for the

charge order state.

From the above the experiment results, it can be concluded that the magnetic memory effect of $\text{Y}_{0.33}\text{Sr}_{0.67}\text{CoO}_3$ compounds arises from the Co^{3+} spin state transition from low to intermediate spin state at a certain temperature. For $\text{Y}_{0.33}\text{Sr}_{0.67}\text{CoO}_3$ sample TGA results¹⁷ suggests that the oxygen stoichiometric is less than 3 and 25% of the Co ions are Co^{4+} , i. e, the most Co ions are Co^{3+} ions. Generally speaking, Co^{3+} ions in air-processed sample are higher than that in O_2 -processed sample. From our structural data we have found there is a difference in the Co-O bond length between the octahedral and tetrahedral sites. This difference is most likely due to the Jahn-Teller effect and the distortion of the octahedral and tetrahedral sites can be a source of the ordering of the orbital. In the $\text{Y}_{0.33}\text{Sr}_{0.67}\text{CoO}_3$ compounds there is an alternation of the octahedral and tetrahedral structure that extends towards the c axes (see Fig. 2). Considering a two dimensional model, along the a direction the spins are aligned in the same direction. Along the b and c direction the spins are aligned in the opposite direction resulting in an antiferromagnetic interaction in the bc plane. It may be noted that such a spin structure supports the fact that there is in-plane ferromagnetic interaction from the Jahn-teller distortion and inter-plane antiferromagnetic interaction from the superexchange interaction. Spin order arrangement of similar kind are also

reported by Roy et al⁹ and Khomskii et al²². There exists a competition between the in-plane ferromagnetic interaction and the inter-plane antiferromagnetic interaction with application of magnetic field and the ferromagnetic interaction overcomes antiferromagnetic superexchange interaction establishing a long range ferromagnetic state at $180 \text{ K} \leq T \leq 304 \text{ K}$ and a cusp with $T_C = 304 \text{ K}$ (see Fig. 4). High magnetic field destroys the Co^{3+} antiferromagnetic state to favor ferromagnetism and both samples suggest the ferromagnetism.

For $\text{Y}_{0.33}\text{Sr}_{0.67}\text{CoO}_3$ sample, the ferromagnetic order is the ground state. According to theory of orbital ordering^{22, 23}, an antiferro-type orbital favors a ferromagnetic order, and a ferro-type orbital order favors an antiferromagnetic order. Suppose the present compound be an insulator consisting of the IS state Co^{3+} , then an orbital order will be an antiferro-type, and prevent the formation of the e_g band, which drives a ferromagnetic order. Similar ferromagnetic states are seen in other orbital-ordered system, such as K_2CuF_4 ²². The stronger orbital order and the decrease of the average $\text{Co}-\text{O}$ bond distance in air-processed sample reduce the thermal activation energy. For air-processed sample, rich Co^{3+} ions results in a higher magnetization and jump temperature than those for O_2 -processede sample.

4. Conclusions

The structure and magnetic properties of air-processed and O_2 -processed $Y_{0.33}Sr_{0.67}CoO_3$ have been outlined. The samples exhibit the type perovskite structure with a space group of I4/mmm (No. 139) and a layered ordering of oxygen vacancies. The alternate layered order of Co-O clusters with CoO_6 octahedron and CoO_4 tetrahedral polyhedron results in the form of the orbital ordering state at 304 K. There is a DC magnetization jump around 200 K (T_J) with a thermal hysteresis under 0.01 T indicating a kind of magnetic memory effects. The appearance of T_J is interpreted as the Co^{3+} spin state transition at a certain temperature from low to intermediate spin state. The thermal hysteresis becomes small and shifts to lower temperature with the increase of the external field, which suggests high magnetic field destroys the Co^{3+} antiferromagnetic and reduces the low ordered temperature. The magnetization transition around 304 K is attributed to the competition of Co^{3+} superexchange anferromagnetic and ferromagnetic interaction. The magnetic measurement suggests the ferromagnetic clusters within an antiferromagnetic matrix are the better model here. The rich Co^{3+} ions and the high orbital ordering state coming from the oxygen deficiency result in the larger magnetization and higher T_J in the air-processed sample. The experimental results show the Co^{3+} spin state transition gives rise to the magnetization jump at around 200 K under

0.01 T.

References

- ¹ F. Fauth, E. Suard, and V. Caignaert, Phys. Rev. B 65, 060401(R) (2001).
- ² P. Ravindran, H. Fjellvag, A. Kjekshus, P. Blaha, K. Schwarz, and J. Luitz, J. Appl. Phys. 91, 291 (2002).
- ³ M. Kriener, C. Zobel, A. Reichl, J. Baier, M. Cwik, K. Berggold, H. Kierspel, O. Zabara, A. Freimuth, and T. Lorenz, Phys. Rev. B 69, 094417 (2004).
- ⁴ N. X. Phuc, N. V. Khiem, and D. N. H. Dao, J. Magn. Magn. Mater. 242-245, 754 (2002).
- ⁵ S. Mukherjee, R. Ranganathan, P. S. Anilkumar, and P. A. Joy, Phys. Rev. B 54, 9276 (1996).
- ⁶ K. Asai, O. Yokokura, N. Nishimori, H. Chou, J. M. Tranquada, G. Shirane, G. Higuchi, S. Okajima, and K. Kohn, Phys. Rev. B 50, 3025 (1994).
- ⁷ S. Tsubouchi, T. Kyomen, M. Itoh, P. Ganguly, M. Oguni, Y. Shimojo, Y. Morii, and Y. Ishii, Phys. Rev. B 66, 052418 (2002).
- ⁸ M. A. Senarís-Rodríguez and J. B. Goodenough, J. Solid State Chem. 118, 323 (1995).
- ⁹ S. Roy, M. Khan, Y. Q. Guo, J. Craig, and N. Ali, Phys. Rev. B 65, 064437 (2002).

¹⁰ J. Wu and C. Leighton, Phys. Rev. B 67, 174408 (2003).

¹¹ C. Zobel, M. kriener, D. Bruns, J. Baier, M. Grüninger, T. Lorenz, P. Reutler, A. Revcolevschi, Phys. Rev. B 66, 020402(R) (2002).

¹² S. Y. Istomin, J. Grins, G. Svensson, O. A. Drozhzhin, E. L. kozhevnikov, E. V. Antipov, and J. P. Attfield, Chem. Mat. 15, 4012 (2003).

¹³ Y. Moritomo, M. Takeo, X. J. Liu, T. Akimoto, and A. Nakamura, Phys. Rev. B 58, R13 334 (1998).

¹⁴ R. H. E. van Doorn and A. J. Burggraaf, Solid State Ionics 128, 65 (2000).

¹⁵ R. L. Withers, M. James, and D. J. Grossens, J. Solid State Chem. 174, 198-208 (2003).

¹⁶ F. Izumi, T. Ikeda, T. Mater. Sci. Froum 2000, 198, 321.

¹⁷ D. J. Goossens, K. F. Wilson, M. James, A. J. Studer and X. L. Wang, Phys. Rev. B 69, 134411 (2004).

¹⁸ Colosal magnetoresistance oxides, edited by Y. Tokura (Gordon & Brench Science Publishers, London, 1999).

¹⁹ P. S. Anil-Kumar, P. A. Joy, and S. K. Date, J. Phys.: Condens. Matter 10, L487 (1998).

²⁰ D. N. H. Nam, K. Jonason, P. Nordblad, N. V. Khiem, and N. X. Phuc, Phys. Rev. B 59, 4189 (1999).

²¹ M. A. Korotin, S. Yu. Ezhov, I. V. Solovyev, V. I. Anisimov, D. I.

Khomskii, and G. A. Sawatzky, Phys. Rev. B 54, 5309 (1996).

²² D. I. Khomskii, and K. I. Kugel, Solid State Commun. 13, 763 (1973).

²³ I. V. Solovyev, Phys. Rev. B 69, 134403 (2004).

Table 1.

Crystal data for O₂-processed Y_{0.33}Sr_{0.67}CoO₃ from the refinement in space group I4/mmm using X-ray diffraction data.

Y _{0.33} Sr _{0.67} CoO ₃	a (Å)	c (Å)	V (Å ³)	2θrange(deg)	S/R _F /R _I
O ₂ -processed	7.6164(2)	15.2747(5)	886.02(5)	5-90°	2.4/4.02/4.83
Air-processed	7.6300(6)	15.284(13)	889.80(13)	5-90°	3.2/4.74/4.86

Selected interatomic distances for Y_{0.33}Sr_{0.67}CoO₃.

Distance (Å)	O2-processed Y _{0.33} Sr _{0.67} CoO ₃	Air-processed Y _{0.33} Sr _{0.67} CoO ₃
Tetrahedron		
Co1-O1(×2)	1.849(6)	1.814(10)
Co1-O2(×2)	1.945(11)	1.978(16)
Co1-O3(×2)	1.925(4)	1.911(8)
Octahedron		
Co2-O1(×2)	2.053(7)	2.144(15)
Co2-O4(×4)	1.910(1)	1.911(1)

Figure Captions

Fig. 1 Least squares fit to the powder X-ray diffraction data collected from O₂-processed Y_{0.33}Sr_{0.67}CoO₃ sample. The dots are experimental data points and the solid line is the calculated. The lower trace shows the difference.

Fig. 2 The refined crystal structure of O₂-processed Y_{0.33}Sr_{0.67}CoO₃ sample.

Fig. 3(a) Magnetization vs temperature curve of O₂-processed Y_{0.33}Sr_{0.67}CoO₃ sample at 0.01 T. (b) Magnetization vs temperature curve of O₂-processed and air-processed samples at 0.01 T. (c) Magnetization vs temperature curve of O₂-processed sample at 0.5 T and 1 T, respectively.

Fig. 4 Zero-field cooled (ZFC) magnetization vs Temperature for O₂-processed Y_{0.33}Sr_{0.67}CoO₃ in fields of 0.01 T and 0.5 T.

Fig. 5(a) M-H loops for air-processed Y_{0.33}Sr_{0.67}CoO₃ sample at 10 K, 210 K and 295 K. (b) M-H loops for O₂-processed Y_{0.33}Sr_{0.67}CoO₃ sample at 10 K, 190 K and 285 K.

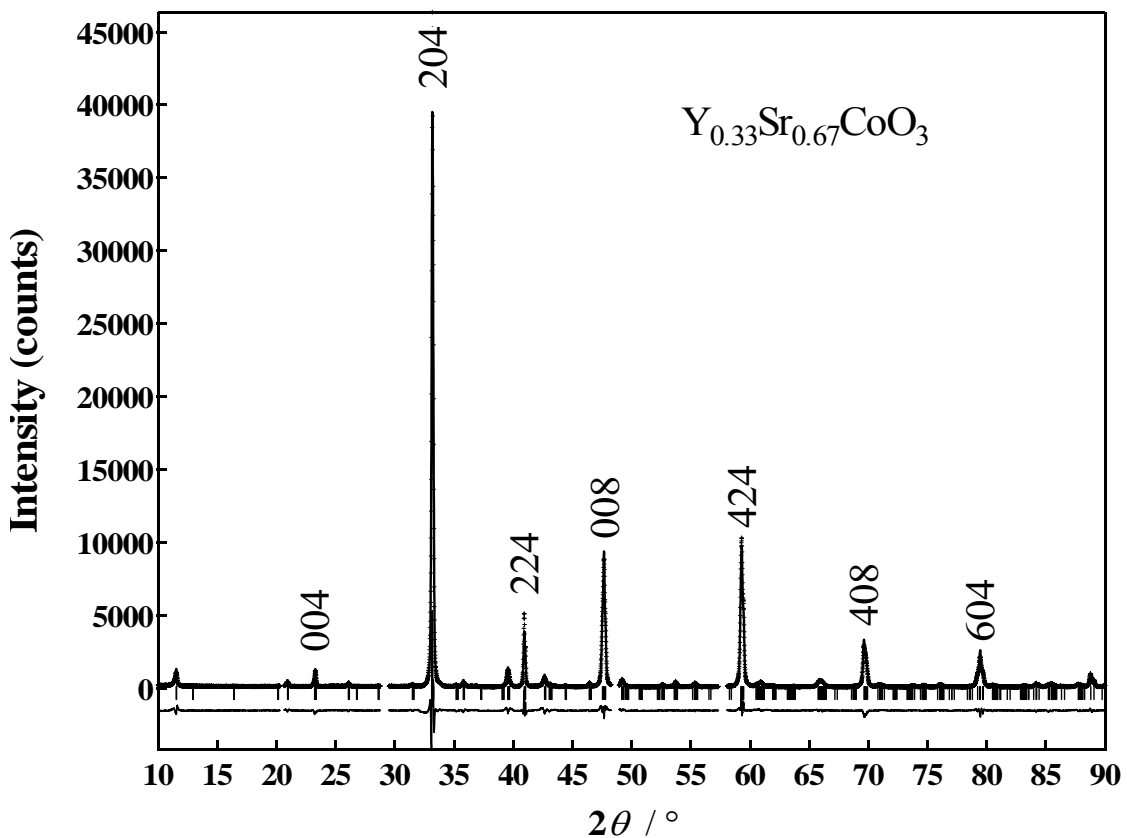


Figure 1. Yufeng Zhang et al.

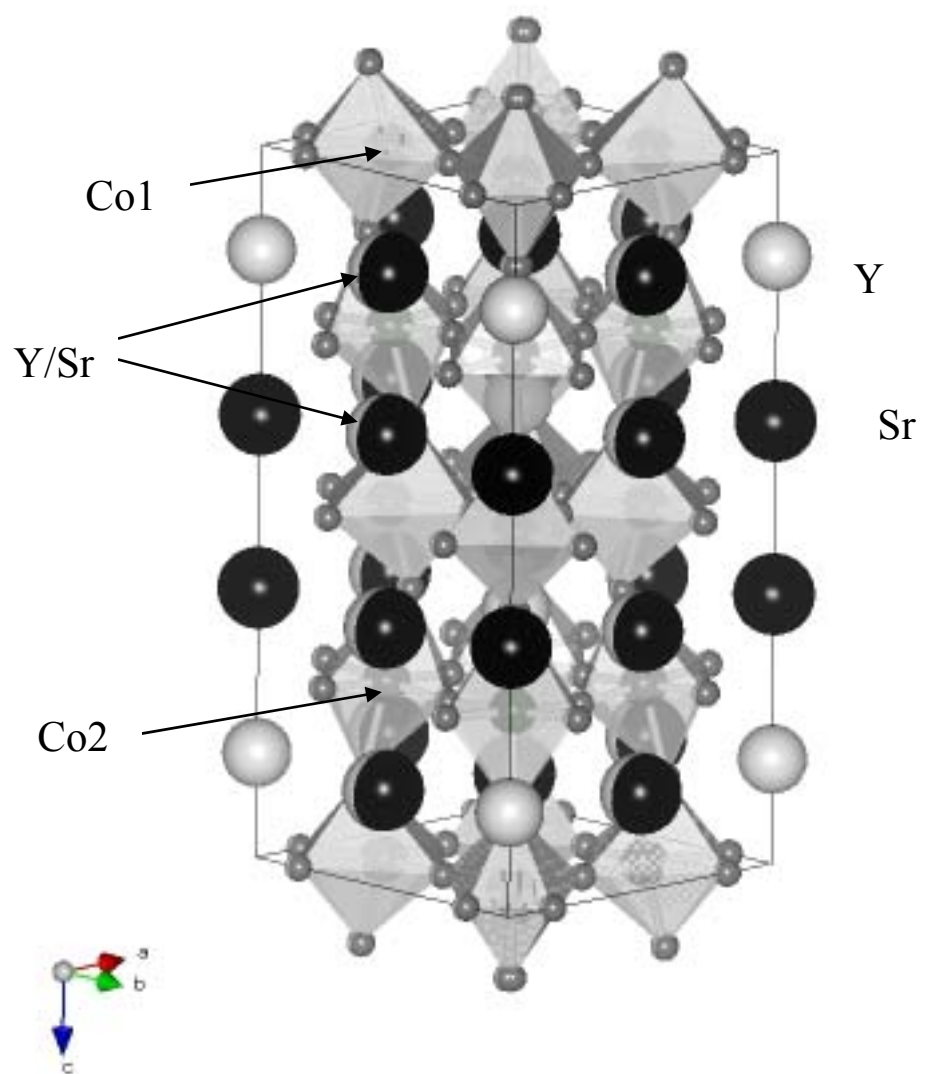


Figure 2. Yufeng Zhang et al.

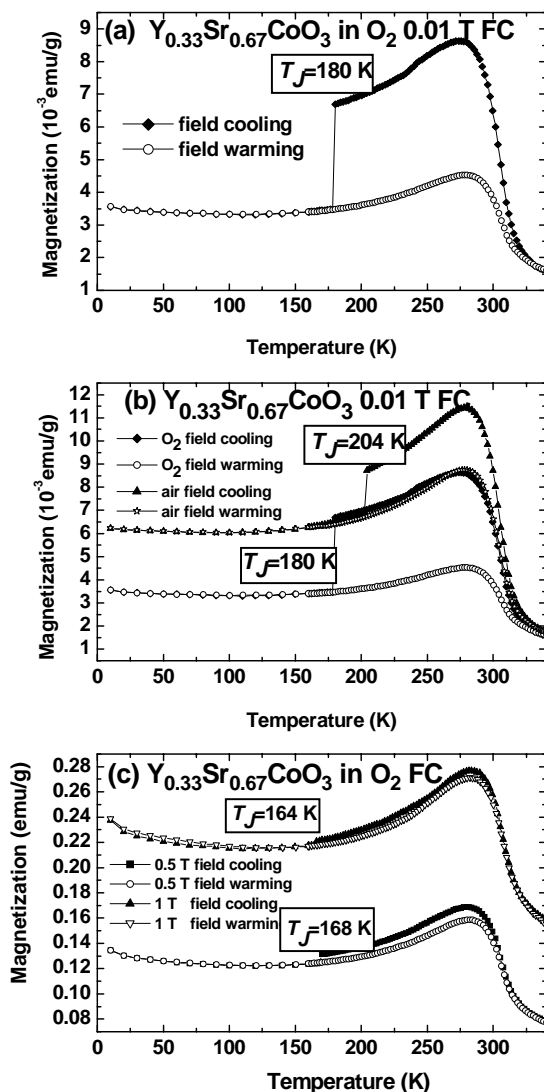


Figure 3(a), (b), (c). Yufeng Zhang et al.

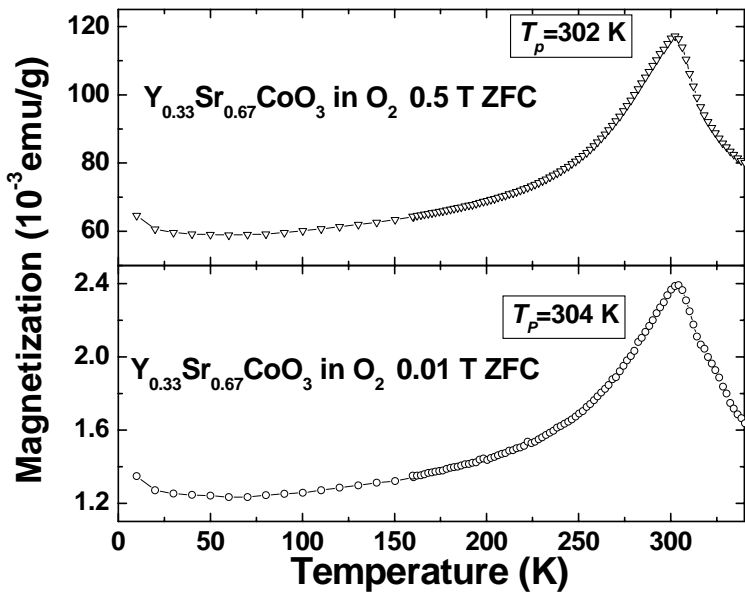


Figure 4. Yufeng Zhang et al.

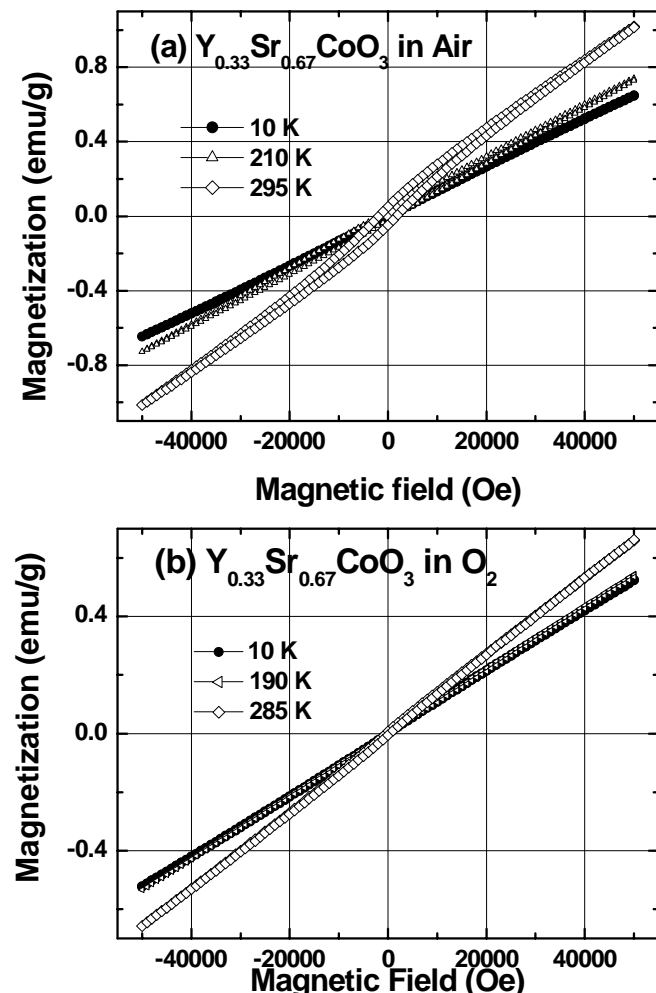


Figure 5(a), (b). Yufeng Zhang et al.